



GEOLOGY AND PETROCHEMISTRY OF GABAL ABU-MESAID AREA, NORTH EASTERN DESERT, EGYPT

L. M. NOSSAIR, A. ABU-DEIF, M. A. EI-TAHIR* and H. I. FARAG

Nuclear Materials Authority, Cairo, Egypt

*Geology Department, South Valley University, Qena, Egypt

(Received: 20 February 2007)

Abstract: A suite of volcanic and plutonic rocks represent the products of Pan-African orogeny; constitute the major litho-tectonic association of Gabal Abu-Mesaid area located in the northern part of the Eastern Desert. These litho-tectonic units are the syn-tectonic older granitoids, mature arc to continental arc Dokhan Volcanics and the associated pyroclastics as well as the widely distributed Post- to late-tectonic younger granites. Almost rock units are invaded by different types of dyke swarms.

The older granitoids are mainly represented by granodiorites that are tectonically described as syn-tectonic plutonites. Geochemically, these rocks are metaluminous, typically I-type that restricted to the pre-late collision stage evolved in a volcanic arc and formed under compressional regime at the lower level of the earth's crust.

Dokhan Volcanics demonstrate a wide spectrum of varieties in which andesites associated with rhyolites and andesitic tuffs, agglomerates as well as ignimbrite are well notified. They are typical calc-alkaline rock series formed in Andean type subduction-related volcanic arc suites. That restricted to the pre-collision stage evolved in a volcanic arc and formed under compressional regime at the lower and middle level of the earth's crust.

Younger granites can be differentiated into two types namely: the fine-grained biotite granites and the medium-to coarse-grained hornblende biotite granites, where these rocks display within plate magmatism, peraluminous calc-alkaline to mild alkaline trend to be potassic affinities.

Introduction

The present work deals with the geology and geochemistry of Gabal Abu-Mesaid area, north Eastern Desert of Egypt (Fig. 1). It was held to accomplish a part of the program of the Nuclear Materials Authority (NMA) of Egypt in carrying out geologic and radiometric survey on the basement rocks to the north of latitude 27° 00' N.

G. Abu-Mesaid area is located between latitudes 27° 17' - 27° 26' N and longitudes 33° 15' - 33° 22' E, covering an area of about 160 km². It is mainly covered with moderate to low rugged hills of late Precambrian rocks, which are unconformably overlain by the Phanerozoic Miocene sediments. The topographic features of the area are, to a large extent, controlled by both of

structural elements and lithology of the different rock units. G. Abu-Mesaid is a NNW-SSE elongated younger granitic intrusion occupying an area of about 80 km².

The area under consideration was previously studied by many authors and included in several studies. Greenberg (1981) mentioned that the younger granites, in the Red Sea hills, are interpreted as three petrographical and geochemical groups characterized by their homogeneity, absence of tectonic foliation, presence of pegmatites and typically low Sr⁸⁷/Sr⁸⁶ ratio.

El-Sharkawy *et al.* (1999) distinguished two contrasting volcanic sequences of G. Dokhan volcanics. The old sequence encompasses slightly metamorphosed (low green facies) andesite flows and their pyroclastics as well as Imperial Porphyry. The young volcanic activity (basaltic and rhyolitic dykes) is tied to an extensional tectonic regime transgressing on the Dokhan Volcanics and the affiliated Hammamat sediments.

El-Kholy *et al.* (1988) carried out geological, geochemical and radioactive studies on some granitoid rocks exposed at the northeastern part of the Qattar batholith. They stated that the contents of the radioelements, U, Th, eU (Ra) and K increase from the older to the younger granites. They added that the Th/U ratio values in the granitoid rocks under consideration are lower than those of the normal granites.

Nossair and El-Gaby (1999) classified the granitic rocks intruding G. Dokhan area into three types; granodiorite, monzogranite and syenogranite. They also stated that the most secondary products are related to the hydrothermal processes that cause silification, chloritization and albitization.

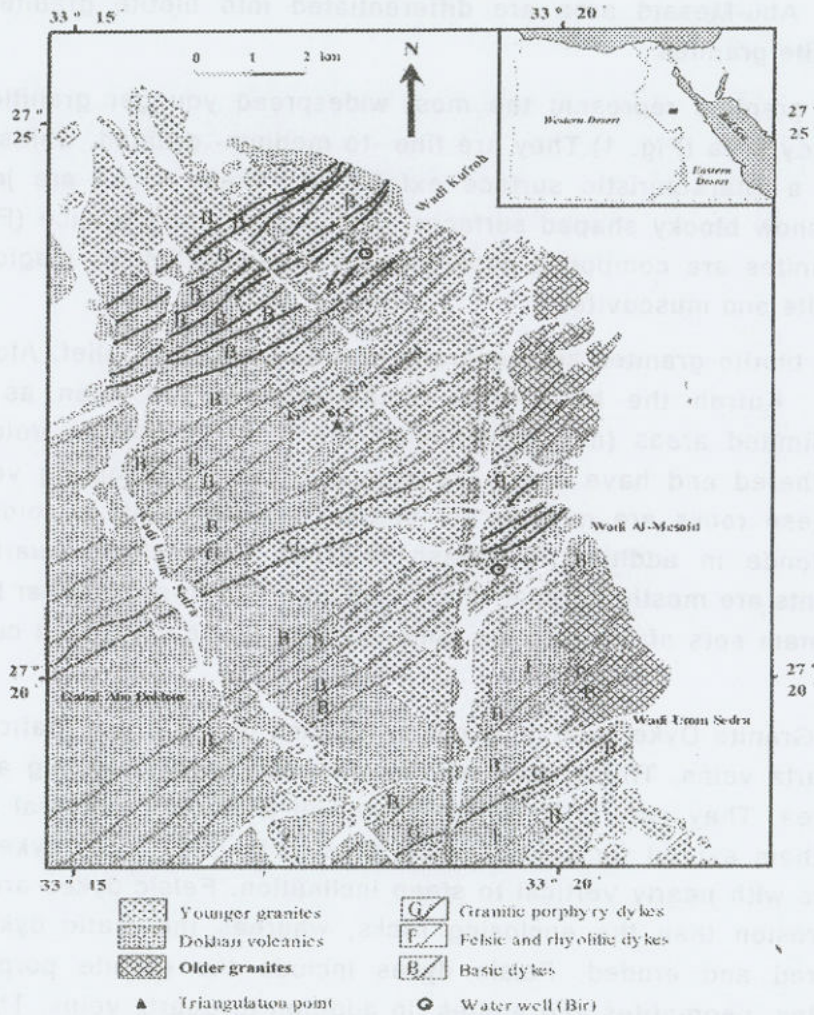
2. GEOLOGIC OUTLINE

G. Abu-Mesaid area is a part of the basement complex of the north Eastern Desert of Egypt. It is mainly covered with an association of plutonic-volcanic rock units. Older granitoids (the oldest), Dokhan Volcanics, younger granites invaded by post-granite dykes (Fig. 1).

2.1. Older Granitoids are restricted to the eastern side of G. Abu-Mesaid pluton as small exposures (about 6 km²) of low -to moderate- topography. They are represented mainly by granodiorite characterized by well developed surface exfoliations. The younger granites of G. Abu-Mesaid intrude these granodiorites through a gradational contact where hybrid contact zones are well developed. On the other hand the contacts between these rocks and Dokhan Volcanics are sharp (Fig. 1&2). Dark-green xenoliths of different shapes and sizes from the older rocks are frequently encountered in the granodiorite masses (Fig. 3). Kaolinitization and epidotization represent the main alteration features.

2.2. Dokhan Volcanics are represented by a thick sequence of lava flows of intermediate to acidic composition, together with a few intercalations of pyroclastics represented mainly by tuffs with locally distributed volcanic

breccias. A few sheets or small lenticular masses of very fine-grained violet ignimbrite are also encountered especially along the eastern periphery of G. Abu-Dokhan. These volcanics are intruded by G. Abu-Mesaid younger granites in the form of large apophyses and offshoots (Fig. 4). The contact between them is everywhere a sharp intrusive contact. These volcanics can be differentiated into two discriminated rock varieties namely andesites with their pyroclastic rocks and felsic volcanic rock.



The andesite eruptions and their pyroclastic rocks form the majority of the Dokhan Volcanics. They are conformably overlain by eruptions of felsic and ash flow tuff sheets. The andesites form a rough country with elevated ridges and narrow rough wadis. Andesites are characterized by porphyritic texture. They are sheared and well jointed. The felsic volcanic rocks form a hilly country with rigid topography, hard, porphyritic, dark grey to purple in colour and show generally a bedding-like appearance.

2.3. Younger granites in G. Abu-Mesaid area intrude the previously described rocks through intrusive sharp contacts and in some places they form hybrid contact zones with the granodiorites. They form the highest mountains, as they are hard and resistant to weathering and erosion. They are jointed (Fig. 5) and dissected by numerous faults and shear zones. The present granites along structural zones become highly hematitized and acquire reddish pink to red colour. These granites contain xenoliths, generally related to previously extrusive Dokhan volcanics indicating their intrusive nature. The Younger granites in G. Abu-Mesaid area are differentiated into biotite granites and hornblende biotite granites.

The biotite granites represent the most widespread younger granitic rock units in the study area (Fig. 1). They are fine -to medium- grained, whitish pink in colour with a characteristic surface exfoliation. These rocks are jointed, fractured and show blocky shaped surfaces with bouldery appearance (Fig. 5). The biotite granites are composed essentially of potash feldspar, plagioclase, quartz and biotite and muscovite.

Hornblende biotite granites are generally of medium to low relief. Along W. Sedra and W. Kufrah the hornblende biotite granites are seen as small exposures of limited areas (non mapable) in the base of Dokhan Volcanics. They are weathered and have sharp contacts with the neighbouring volcanic sequences. These rocks are medium to -coarse- grained, pink in colour and contain hornblende in addition to potash feldspar, plagioclase, quartz and biotite. The joints are mostly vertical which may give rise to rectangular blocky, following the main sets of intersecting joints as well as bouldery and cupoidal blocks.

2.4. The Post Granite Dyke Swarms occur as swarms of felsic and mafic dykes as well as quartz veins. These dyke swarms are post granitic cutting all rock units in the area. They vary in thickness from half a meter to several meters and some of them extend for several kilometres in length. These dykes form parallel swarms with nearly vertical to steep inclination. Felsic dykes are more resistant to erosion than the enclosing rocks, whereas the mafic dykes are easily weathered and eroded. Felsic dykes include the granite porphyries, rhyolites, felsites, pegmatites and aplites, in addition to quartz veins. They are mostly running in NE-SW, E-W and NW-SE directions. Mafic dykes are represented by andesite, dolerite and basalt. They are mostly running in NE-SW, E-W and N-S directions.

3. PETROGRAPHIC FEATURES

3.1. Granodiorites is a holocrystalline, equigranular and shows hypidiomorphic textures. It is composed of plagioclase, K- feldspar; quartz, hornblende and biotite. Zircon and apatite are the main accessory minerals.

Plagioclase occurs as subhedral to euhedral tabular crystals, exhibiting both lamellar and simple twinning. Zoned crystals are common; with poikilitic inclusions of quartz and biotite (Fig. 6). Potash feldspars are mainly represented by orthoclase and microcline perthites; in which the orthoclase perthite is more dominant. They occur as subhedral to euhedral crystals. Orthoclase perthite poikilitically encloses plagioclase and biotite (Fig. 7) is usually kaolinized and rarely exhibits twinning due to its alteration. Microcline exhibits cross-hatching twinning. Quartz occurs as subhedral to anhedral crystals, corroding and infiltrating the other constituents. Some crystals show undulose extinction, highly cracked. It occasionally includes apatite, zircon, and iron oxides and frequently dusted with iron oxides and clay minerals especially along peripheries. Biotite is strongly pleochroic from pale to dark brown. Inclusions of zircon, apatite, sphene, quartz and iron oxides are commonly observed. It is partly altered to chlorite with releasing iron oxides especially along cleavage planes. Their cleavage planes are sometimes kinked due to the deformational processes. Hornblende is less dominant than biotite. It forms dark green anhedral -to subhedral- crystals and occasionally shows simple twinning. It encloses small plagioclase and quartz crystals giving poikilitic texture. Some hornblende crystals are partly altered to chlorite. It also forms clusters associated with biotite, iron oxides and sphene.

3.2. Dokhan Volcanics The present Dokhan Volcanic rocks are classified into two main rock types namely: lava flows (andesite porphyry, devitrified and glassy rhyolites) and pyroclastics (andesitic banded tuffs, andesitic lithic crystal tuffs, andesitic crystal lapilli's tuffs, ignimbrite and andesitic agglomerates), which are described as follows.

The Dokhan volcanics comprise a wide spectrum of lava flows (andesitic to acidic varieties) with abundant andesite porphyries. These lavas exhibit different textures characterizing the stages of the flows. The common textures present are porphyritic (Fig. 8). The main alteration processes affected these rocks are chloritization, sericitization, and silicification. Pyroclastic rocks are interlayer with the volcanic flows and are more abundant than them. They include ash flow tuffs, crystal tuffs and lapilli's tuffs and agglomerates. Welded acidic tuffs or ignimbrite are recorded (Fig. 9).

3.3. Younger Granites

3.3.1. Biotite granites

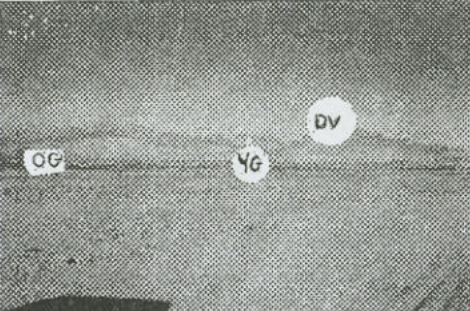


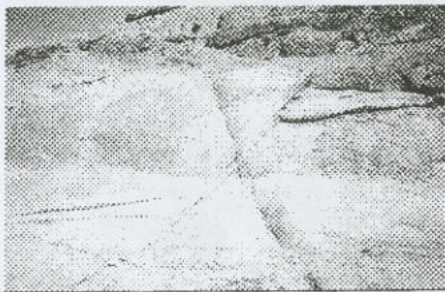

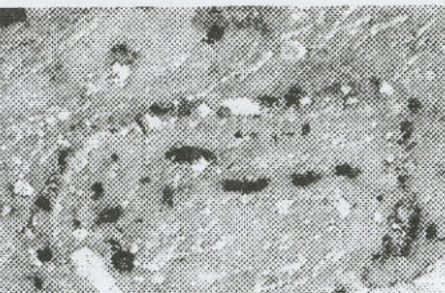
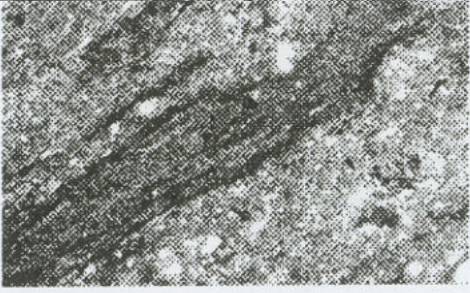

Biotite granites are composed essentially of perthites, plagioclase, quartz, and biotite. Apatite, muscovite, zircon, sphene and opaques are the accessory minerals. Sericite, kaolinite, epidote and chlorite occur as secondary minerals.

Perthites occur as subhedral to euhedral crystals. They are represented by orthoclase and microcline perthites. Orthoclase perthite commonly shows simple twinning and slightly kaolinized and sericitized. Secondary albite rims due to the Na-exsolved from the potash host rock replace some perthite

crystals giving rise to rapakivi texture (Fig. 10). Quartz occurs as anhedral to subhedral crystals with various sizes and form inter-looking between feldspar. It exhibits strong wavy extinction and is intergrown with the K-feldspars forming graphic textures. Plagioclases occur in subordinate amounts as euhedral to subhedral prismatic crystals. They display lamellar twinning and normal zoning (Fig. 11). Two phases of plagioclase are recognized. The first phase is small in size and enclosed poikilitically in perthite and biotite. The second one includes large plagioclase crystals, which are corroded by perthite. Biotite represents the main mafic minerals in the rock. It occurs as subhedral flakes, brown colour and displays strong pleochroism. It is altered to chlorite accompanied by opaques (Fig. 12) especially along crystal borders. It encloses crystal of apatite and iron oxides. Sphene occurs as euhedral sphenoidal shaped crystals enclosed mainly in quartz (Fig. 13). Zircon usually occurs as minute euhedral tabular crystals with high relief and often colourless enclosed within feldspars and quartz. It also occurs as inclusions in biotite, where they form pleochroic halos (Fig. 14). Apatite is rarely encountered as thin colourless prismatic crystals characterized by a moderate relief and first order interference colours. Iron oxides occur as subhedral to anhedral grains associated generally with the mafic minerals.

3.3.2. Hornblende biotite granites. Petrographically, the hornblende biotite granites exhibit porphyritic and some show hypidiomorphic textures. They are essentially composed of alkali feldspar, plagioclase, quartz, hornblende and biotite. Zircon, apatite, sphene and opaque are the main accessories whereas chlorite, sericite and kaolin are secondary minerals.

The alkali feldspars encompass orthoclase and microcline perthites. They occur as subhedral to anhedral crystals. Orthoclase perthite and microcline perthite are corroded by quartz (Fig. 15). Alkali feldspars are cloudy due to kaolinitization. Simple twinning is common. They display string perthitic and occasionally graphic intergrowths. Non-perthitic microcline is rarely present as minute intergranular crystals, most probably developed due to a phase of k-metasomatism quite latter than the crystallization of the granite. Plagioclases occur as subhedral-anhedral crystals of variable sizes. Distinct lamellar twinning and zoning (Fig. 16) of both normal and oscillatory types are observed. Sometimes, they are encircled by myrmekitic quartz rims especially along crystal borders. Plagioclase suffers slight sericitization especially at crystal cores. Quartz occurs as anhedral inter-looking crystals between the feldspar minerals. The crystals are inclusions-rich and exhibit strained undulatory extinction. Hornblende occurs as subhedral crystals of green colour. Both biotite and sphene usually surround them. The hornblende suffers slightly chloritization especially along crystal borders (Fig. 17). Biotite occurs as subhedral crystals. The crystals are brown in colour and display strong pleochroism. Biotite crystals suffer partially alteration though chloritization.

	
<p>Fig. (2): Panoramic view showing Dokhan Volcanics (DV), younger granites (YG) and older granitoids (OG), G. Abu-Mesaid area, looking W</p>	<p>Fig. (3): Close-up view showing xenoliths of metavolcanics enclosed within granodiorites, G. Abu-Mesaid area</p>
	
<p>Fig. (4): An offshoot of younger granites (YG) in Dokhan volcanics, G. Abu-Mesaid area, looking E</p>	<p>Fig. (5): Coarse-grained biotite granites exhibiting highly jointed, G. Abu-Mesaid area, looking NW</p>
	
<p>Fig. (6): photomicrograph of granodiorite showing fine crystals of quartz and biotite poikilitically enclosed in plagioclase, G. Abu-Mesaid area, C.N.X8</p>	<p>Fig. (7): photomicrograph in granodiorite showing megacryst of orthoclase perthite engulfing plagioclase and biotite, G. Abu-Mesaid area, C.N.X8</p>
	
<p>Fig. (8): photomicrograph of ignimbrite showing fluidal texture, G. Abu-Mesaid area, C.N.X8</p>	<p>Fig. (9): photomicrograph of andesite porphyry showing porphyritic texture with cubic crystal of iron oxide, G. Abu-Mesaid area, C.N.X8</p>


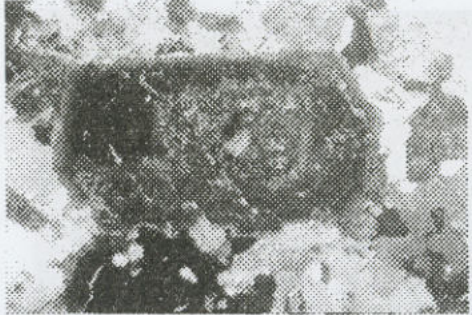
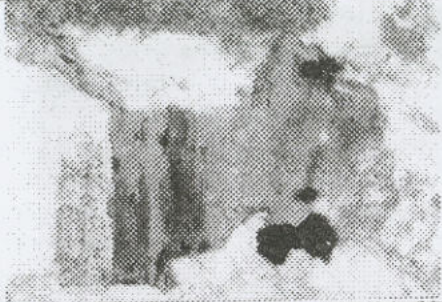





	
<p>Fig. (10): photomicrograph of biotite granites showing rapakivi texture, G. Abu-Mesaid area, C.N.X8.</p>	<p>Fig. (11): photomicrograph of biotite granites showing zoned plagioclase crystal, G. Abu-Mesaid area, C.N.X10.</p>
	
<p>Fig. (12): Photomicrograph of biotite granites showing biotite flakes altered to chlorite with liberation of iron oxides along peripheries, G. Abu Mesaid area, C.N.X 16.</p>	<p>Fig. (13): Photomicrograph of biotite granite showing sphene crystal associated with iron oxide, G. Abu Mesaid area, C.N.X 16.</p>
	
<p>Fig. (14): Photomicrograph of biotite granites showing metamict zircon crystal, G. Abu Mesaid area, C.N.X32.</p>	<p>Fig. (15): Photomicrograph of hornblende biotite granite showing orthoclase perthite and microcline perthite corroded by quartz, G. Abu Mesaid area, C.N.X8.</p>
	
<p>Fig. (16): Photomicrograph of hornblende biotite granites showing zoned plagioclase crystal, G. Abu Mesaid area, C.N.X10.</p>	<p>Fig. (17): Photomicrograph of hornblende biotite granite showing elongated hornblende crystal corroded by biotite and sphene, G. Abu Mesaid area, C.N.X10</p>

Table (1): Major oxides (Wt %) and trace elements (ppm) analyses of Abu Mesaid Dokhan Volcanics

Rock	Andesite								Ignembrite					
Sample	14B	15B	43A	89	94	99	103	avg.	94A	94B	96A	96B	97A	avg.
a) Major oxides (Wt%)														
SiO ₂	60.10	61.20	59.15	59.10	60.90	61.10	60.00	60.22	73.30	73.40	73.29	73.60	73.10	73.34
TiO ₂	1.10	1.30	1.25	1.20	1.25	1.15	1.30	1.22	0.60	0.40	0.48	0.40	0.55	0.49
Al ₂ O ₃	15.80	15.70	15.25	18.30	16.00	16.15	15.40	16.09	13.16	13.02	13.17	13.10	13.15	13.12
Fe ₂ O ₃	5.70	5.60	6.45	5.30	5.55	5.52	0.50	4.95	2.50	2.15	2.13	2.10	2.35	2.25
MnO	0.07	0.08	0.15	0.08	0.06	0.15	0.11	0.10	0.06	0.07	0.07	0.06	0.07	0.07
MgO	5.50	4.70	5.15	3.05	4.30	4.10	4.55	4.48	1.25	1.18	1.17	1.19	1.22	1.20
CaO	6.25	6.05	6.35	6.80	5.80	5.60	6.10	6.14	1.15	1.23	1.19	1.26	1.20	1.21
Na ₂ O	3.50	3.10	3.45	3.05	3.25	3.40	3.80	3.36	4.02	4.18	4.14	4.14	4.20	4.14
K ₂ O	1.10	1.25	1.80	1.75	1.50	1.65	1.20	1.46	3.30	3.35	3.35	3.30	3.40	3.34
P ₂ O ₅	0.32	0.35	0.32	0.35	0.40	0.34	0.36	0.35	0.14	0.12	0.20	0.14	0.16	0.15
L.O.I	0.59	0.61	0.63	0.93	0.95	0.82	0.65	0.74	0.51	0.88	0.46	0.69	0.58	0.62
Total	100.0	99.99	99.99	99.99	99.99	99.97	99.99		99.99	99.98	99.99	99.98	99.98	99.98
CIPW norm values														
Q	14.49	18.21	13.78	16.10	19.01	18.32	14.22	16.30	33.44	32.31	31.22	33.05	31.89	32.38
Or	13.68	12.51	13.70	12.25	8.96	9.84	11.91	11.84	19.64	19.87	19.92	19.66	20.23	19.86
Ab	27.20	26.38	26.80	26.04	27.74	28.98	32.34	27.93	34.19	35.45	37.47	35.24	35.71	35.61
An	22.04	22.82	20.78	30.45	24.85	24.09	19.15	23.45	4.92	5.37	4.76	5.41	5.05	5.10
C	0.00	0.00	0.00	0.00	0.00	0.00	0.00	0.00	1.18	0.55	0.55	0.74	0.71	0.75
Di	3.70	2.18	6.94	0.54	1.45	0.00	5.31	2.87	0.00	0.00	0.00	0.00	0.00	0.00
hy	12.13	10.82	9.75	7.46	10.19	14.44	9.00	10.54	3.14	2.48	2.95	3.00	3.07	2.93
mt	0.23	0.26	0.49	0.26	0.20	0.49	0.36	0.33	0.20	0.23	0.23	0.20	0.23	0.22
he	5.58	5.46	6.15	5.17	5.47	5.31	6.29	5.63	2.38	2.01	1.99	1.98	2.21	2.11
ap	0.70	0.77	0.70	0.77	0.88	0.75	0.79	0.77	0.31	0.26	0.44	0.33	0.35	0.34
b) Trace elements (ppm)														
Ba	225	240	235	227	260	230	255	238.86	470	480	475	465	485	475.00
Rb	40	37	39	41	38	40	36	38.71	190	205	198	200	201	198.80
Sr	200	210	225	205	220	210	230	214.29	123	125	121	130	127	125.20
Y	19	22	20	25	20	21	23	21.43	30	28	26	32	31	29.40
Zr	130	122	125	127	121	128	120	124.71	180	192	177	190	185	184.80
Nb	5	6	5	4	5	5	4	4.86	29	29	30	28	31	29.40
Pb	30	26	22	26	31	33	28	28.00	25	30	27	28	26	27.20
Ga	18	23	20	16	11	28	23	19.86	13	13	26	12	13	15.40
Cu	18	19	18	17	20	19	17	18.29	35	39	36	38	37	37.00
Ni	28	29	31	26	30	27	34	29.29	2	2	3	2	3	2.40
Differentiation index														
D.I.	55.37	57.10	54.28	54.39	55.71	57.14	58.47	56.07	87.27	87.63	89.61	87.95	87.83	88.06

4. GEOCHEMISTRY

Thirty-three representative samples were chemically analyzed for major oxides and trace elements. The major oxides and trace elements were determined using XRF techniques at the laboratory of the Nuclear Materials Authority (NMA) in Cairo. The results are listed in table (1) for the Dokhan Volcanics and table (2) for both granitoid rocks.

4.1. Geochemistry of Dokhan Volcanics

The major oxides of the Dokhan Volcanics show two isolated ranges; the first is characterized by silica content ranging from 59.10% to 61.20% (avg. 60.22) and the other ranges from 73.10% to 73.60% (avg.73.34) corresponding to andesite and ignimbrite respectively. Andesites are characterized by relatively higher TiO_2 content accompanied with high Al_2O_3 , FeO, MgO and CaO while the other oxides are low rather than those of ignimbrite which is characterized by higher K_2O and Na_2O contents. Andesite is also characterized by higher Sr only while the ignimbrite has higher values for Rb, Nb, Ba, Zr (Table 1).

The differentiation index D.I. as a measure of the leucocratic nature of igneous rocks (Thronton and Tuttle, 1960), is low in andesite (ranges from 54.28 to 58.47) and higher in ignimbrite (range from 87.27 to 89.61). Within each rock type the D.I. values show a very narrow range reflecting a considerable degree of homogeneity.

Classification and magma type: By using the SiO_2 - Zr/ TiO_2 classification diagram (Winchester and Floyd, 1977), the samples are characterized by low silica content and low Zr/ Ti_2O ratio falls in the andesite field, while those with higher values (ignimbrite) falls in the rhyolite field classifying them into intermediate and acidic Dokhan volcanics (Fig. 18). On the total alkali- SiO_2 diagram (Irvine and Baragar, 1971), all the studied samples plot in the subalkaline field (Fig. 19) indicating orogenic magmatism and calc-alkaline nature.

Tectonic setting: Plotting of the studied volcanics on the Zr/4-Nb*2-Y discrimination diagram (Meschede, 1986) clarified that the andesite samples plot in the volcanic arc basalt field (Fig. 20).

4.2. Geochemistry of granitic rocks

The major oxides of the granites under consideration showed three isolated ranges; the first is characterized by silica content ranging from 66.10% to 66.66%, the second ranges from 71.10% to 71.80% and the third ranges from 72.68 to 73.57, corresponding to granodiorite, hornblende-biotite granite and biotite granite respectively. Granodiorite samples are characterized by relatively higher Al_2O_3 content accompanied with high FeO, MgO and CaO and P_2O_5 contents. The other oxides are low rather than those of the younger granites (hornblende-biotite granite and biotite granite) which are characterized by higher K_2O and Na_2O contents, specially the biotite granite which shows the highest K_2O content. Granodiorite is also characterized by higher Ba, Sr, Cu and V while the younger granites have higher values for Rb, Nb, Zr especially the biotite granite which shows the highest values (Table 2).

The differentiation index (D.I.) values of older granitoids are relatively low (72-74) compared with those of younger granites (90-94); these high values indicate highly differentiated magma. Figures (21&22) show the relation between major and trace elements of the examined rocks versus D.I. values. In these figures, there is a compositional gap between the older granitoids and

younger granites which were derived from independent magma. It can be noticed that both SiO_2 and K_2O contents increase from granodiorites to younger granites. This increase is justified by the modal increase of quartz and alkali feldspar while Al_2O_3 , CaO , Fe_2O_3 and MgO decrease in the same direction due to the increase of mafic mineral contents. On the other hand, the trace elements Y, Rb, Nb and Zr show positive scorrrelation with D.I. while Sr and Ba show negative correlation.

Classification and magma type: The granitic rocks of the studied area could be classified geochemically by using the Or-Ab-An classification diagram (Streckeisen 1976). It shows that the older granitoids which are characterized by the higher anorthite content fall within the granodiorite field while the biotite granite samples are mostly syenogranite and the hornblende-biotite granite samples are monzogranite (Fig. 23). Plotting of the same samples on the SiO_2 - Al_2O_3 -Alk ternary diagram (MacDonald and Bailey, 1973) verified that all the studied granitoids are of calc-alkaline nature (Fig. 24).

Tectonic Setting: Plotting of the studied granitoids on Shand's index diagram (Maniar and Piccoli, 1989) clarified that the studied older granitoids plot in the metaluminous field (Fig.25), whereas the younger granites plot in the peraluminous field. The peraluminous nature is deduced of the presence of ferromagnesian minerals. The plotting of older granitoids in metaluminous field indicates magma generation within a nature thickened crust typical for magmatic suites of igneous source (Debon and Le Fort, 1983). On the SiO_2 - Al_2O_3 discrimination diagram (Maniar and Piccoli, 1989), the studied younger granites plot in the POG field (Fig. 26). Using Nb-Y discrimination diagram (Pearce *et al.*, 1984) clarified that the studied older granitoids plot in volcanic arc granitoids field (VGA), while the younger granite (Fig. 27) plots clearly in within-plate granites field (WPG)

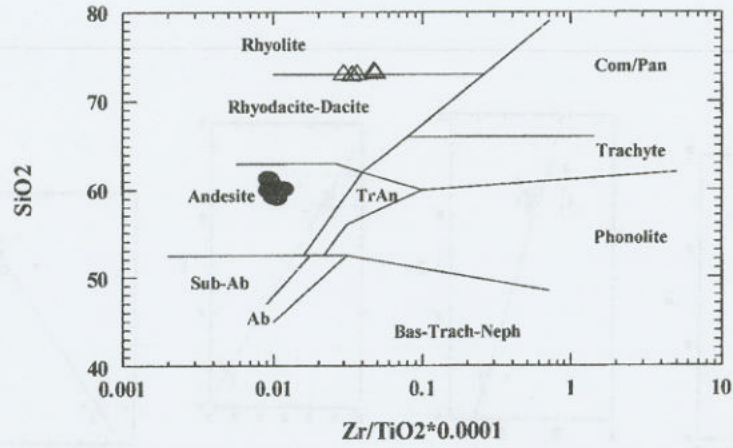
Conclusion

The previous field work and petrochemical characteristics indicate the following concluding remarks:

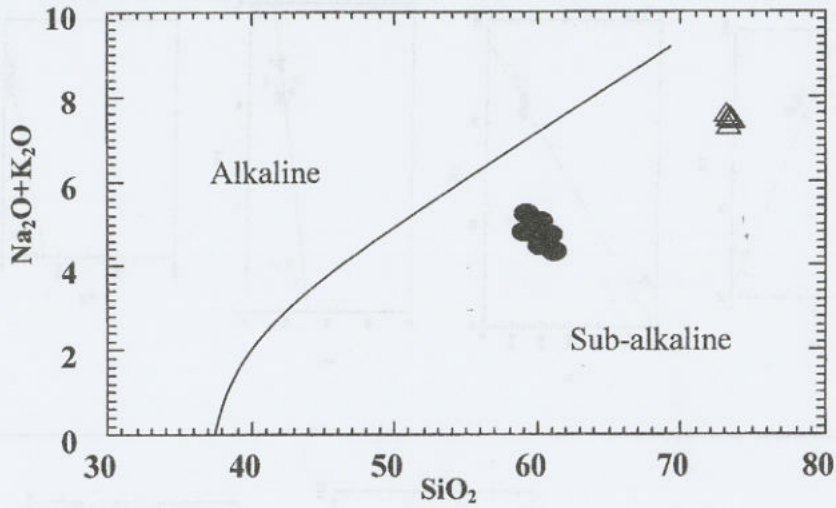
- 1- Gabal Abu-Mesaid area is dominated by older granitoids (the oldest rock unit), Dokhan Volcanics and younger granites (the youngest). These rocks are invaded by post-granite dykes.
- 2- The volcanics dominating the area are intermediate and acidic Dokhan described as andesite and ignimbrite (rhyolite).
- 3- The Dokhan volcanics are characterized by K/Rb ratios ranging from 135 to 383 with an average value 240. This value is somewhat similar to the normal average (250) given by Taylor (1965), suggesting derivation from mantle source regions that were Rb-enriched. Tectonic setting of the studied Dokhan Volcanics clarified that the andesite samples plot in the volcanic arc basalt field.

Table (2): Major oxides (Wt%) and trace elements (ppm) analyses of Abu Mesaïd granites.

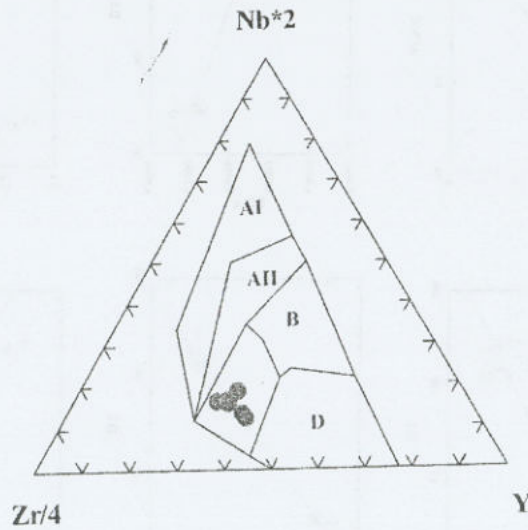
Rock	Older Granites												Younger Granites													
	Granodiorite						Hornblende-biotite granite						Biotite granite													
Sample	46A	48	67	69	70	79A	avg.	12	17	101	102	105	avg.	22	26A	33	36	43	45	49	51	79	80	avg.		
a) Major oxides (Wt%)																										
SiO ₂	66.10	66.66	66.40	66.20	66.10	66.20	66.28	71.65	71.60	71.80	71.80	71.51	71.67	72.68	73.37	72.60	73.70	72.45	72.55	73.05	72.40	72.30	73.57	72.87		
TiO ₂	0.30	0.18	0.22	0.25	0.28	0.24	0.25	0.20	0.20	0.18	0.19	0.18	0.19	0.18	0.16	0.15	0.18	0.17	0.19	0.15	0.19	0.19	0.16	0.17		
Al ₂ O ₃	14.30	14.95	14.51	14.20	14.20	14.36	14.42	13.20	14.20	13.87	13.55	13.40	13.64	13.30	13.20	13.25	13.25	13.00	13.20	13.15	13.20	13.30	13.1	13.20		
Fe ₂ O ₃	3.45	3.13	3.45	3.40	3.45	3.45	3.39	2.36	2.30	2.40	2.50	2.75	2.46	2.40	2.30	2.70	2.40	2.70	2.50	2.51	2.60	2.80	2.6	2.55		
MnO	0.10	0.20	0.09	0.09	0.07	0.08	0.11	0.08	0.07	0.07	0.07	0.06	0.07	0.05	0.05	0.04	0.06	0.06	0.07	0.04	0.07	0.05	0.04	0.05		
MgO	2.15	1.23	2.00	2.30	2.35	2.30	2.06	0.55	0.60	0.35	0.60	0.55	0.53	0.50	0.40	0.44	0.39	0.45	0.70	0.40	0.55	0.55	0.4	0.48		
CaO	5.25	5.30	4.65	4.70	4.87	4.98	4.96	1.45	1.35	1.50	1.70	1.30	1.46	1.15	0.90	1.10	0.95	1.35	1.50	0.69	1.60	1.18	0.7	1.11		
Na ₂ O	4.27	4.12	4.15	4.22	4.25	4.10	4.19	4.65	4.58	4.55	4.85	4.70	4.67	4.70	4.08	4.65	4.29	4.68	4.61	4.22	4.51	4.45	4.29	4.45		
K ₂ O	3.41	3.09	3.35	3.30	3.40	3.32	3.31	4.44	4.42	4.35	4.63	4.72	4.51	4.30	5.25	4.55	5.15	4.45	4.55	5.20	4.28	4.44	5.45	4.76		
P ₂ O ₅	0.32	0.09	0.36	0.30	0.34	0.28	0.28	0.13	0.12	0.13	0.15	0.16	0.14	0.10	0.09	0.15	0.09	0.11	0.10	0.12	0.13	0.17	0.13	0.12		
L.O.I	0.55	0.98	0.59	0.57	0.68	0.56	0.66	0.72	0.64	0.78	6.00	0.61	1.75	0.55	0.78	0.45	0.51	0.56	0.60	0.52	0.47	0.52	0.46	0.54		
Total	100.0	99.99	99.99	99.99	99.99	99.98	99.98	99.98	100.0	99.99	99.99	100.0	99.99	99.99	99.99	99.98	99.99	99.98	99.99	99.99	100.0	99.99	99.99	99.99		
CIPW norm values																										
q	17.76	19.58	19.39	18.99	18.14	19.21	18.85	24.86	24.94	26.01	22.91	23.78	24.50	26.71	27.74	26.19	27.11	27.52	25.47	27.21	26.98	26.96	26.28	26.82		
or	20.24	18.28	19.94	19.72	20.25	19.82	19.71	26.46	26.28	25.93	27.57	28.14	26.88	25.60	31.11	27.02	30.32	26.74	26.92	30.91	25.45	26.44	26.10	28.26		
ab	36.22	34.86	35.29	36.04	36.17	34.98	35.59	39.59	39.91	38.75	41.26	40.50	40.00	39.98	34.54	39.46	36.09	40.19	38.97	35.85	38.32	37.86	36.10	37.74		
an	9.78	13.19	11.10	10.13	9.66	10.60	10.74	3.52	5.21	4.75	1.50	1.23	3.24	2.47	2.16	1.81	1.64	1.11	1.85	1.55	3.11	3.19	0.35	1.92		
di	11.26	6.71	7.63	9.07	9.85	9.52	9.01	2.31	0.71	1.68	3.26	2.98	2.19	2.08	1.39	2.16	1.97	2.44	3.78	0.93	2.98	1.32	2.05	2.11		
hy	0.18	0.00	6.48	1.61	1.36	1.38	1.84	0.32	1.18	0.10	0.00	0.00	0.32	0.29	0.36	0.10	0.06	0.00	0.00	0.58	0.00	0.77	0.04	0.22		
mt	0.33	1.96	0.30	0.30	0.23	0.26	0.56	0.26	0.23	0.23	0.23	0.20	0.23	0.16	0.16	0.13	0.20	2.58	0.23	0.13	0.23	0.16	0.13	0.41		
he	3.24	3.07	3.21	3.23	3.32	3.29	3.23	2.20	2.17	2.26	2.36	2.63	2.32	2.30	2.19	2.62	2.25	0.00	2.34	2.43	2.45	2.70	2.49	2.18		
ll	0.00	0.00	0.00	0.00	0.00	0.00	0.00	0.00	0.00	0.00	0.00	0.00	0.00	0.00	0.00	0.00	0.00	0.00	0.00	0.00	0.00	0.00	0.00	0.00		
ap	0.70	0.21	0.79	0.66	0.75	0.71	0.64	0.29	0.35	0.35	0.33	0.24	0.31	0.22	0.26	0.24	0.22	0.24	0.22	0.20	0.18	0.18	0.28	0.22		
b) Trace elements (ppm)																										
Ba	648	624	762	560	654	552	633	500	488	450	435	445	464	515	420	448	395	484	462	422	471	499	415	453.10		
Rb	35	31	37	31	38	36	35	30	31	28	29	32	30	128	105	177	120	172	145	155	138	189	160	148.90		
Sr	422	150	570	557	509	550	460	120	127	125	130	128	126	130	106	129	99	131	137	96	121	122	102	117.30		
Y	23	10	10	38	29	25	23	30	31	28	29	32	30	91	89	85	111	82	105	99	89	86	113	95.00		
Zr	61	64	50	54	75	108	69	144	140	148	150	160	148	140	121	208	127	215	124	185	205	220	211	175.60		
Nb	13	18	16	9	17	15	15	65	65	68	73	75	69.2	96	80	115	88	112	98	100	105	120	107	102.10		
Pb	16	20	18	14	18	17	17	54	58	58	56	58	56.8	57	45	55	59	48	53	67	48	67	65	56.40		
Ga	19	22	20	20	17	45	24	19	17	18	21	22	19.4	14	18	21	18	15	17	17	17	18	20	18	17.60	
Cu	13	22	43	32	12	259	64	11	11	12	11	14	11.8	9	12	11	14	11	10	10	15	12	10	14	11.80	
V	57	45	59	47	42	46	49	11	13	13	10	12	11.8	9	7	11	7	18	24	10	11	8	11	11.60		
Differentiation index																										
D.I.	74.22	72.72	74.62	74.75	74.56	74.01	74.15	90.91	90.69	90.69	91.74	92.42	91.3	92.29	93.39	92.67	93.52	94.45	91.36	93.97	90.75	91.26	94.48	92.81		



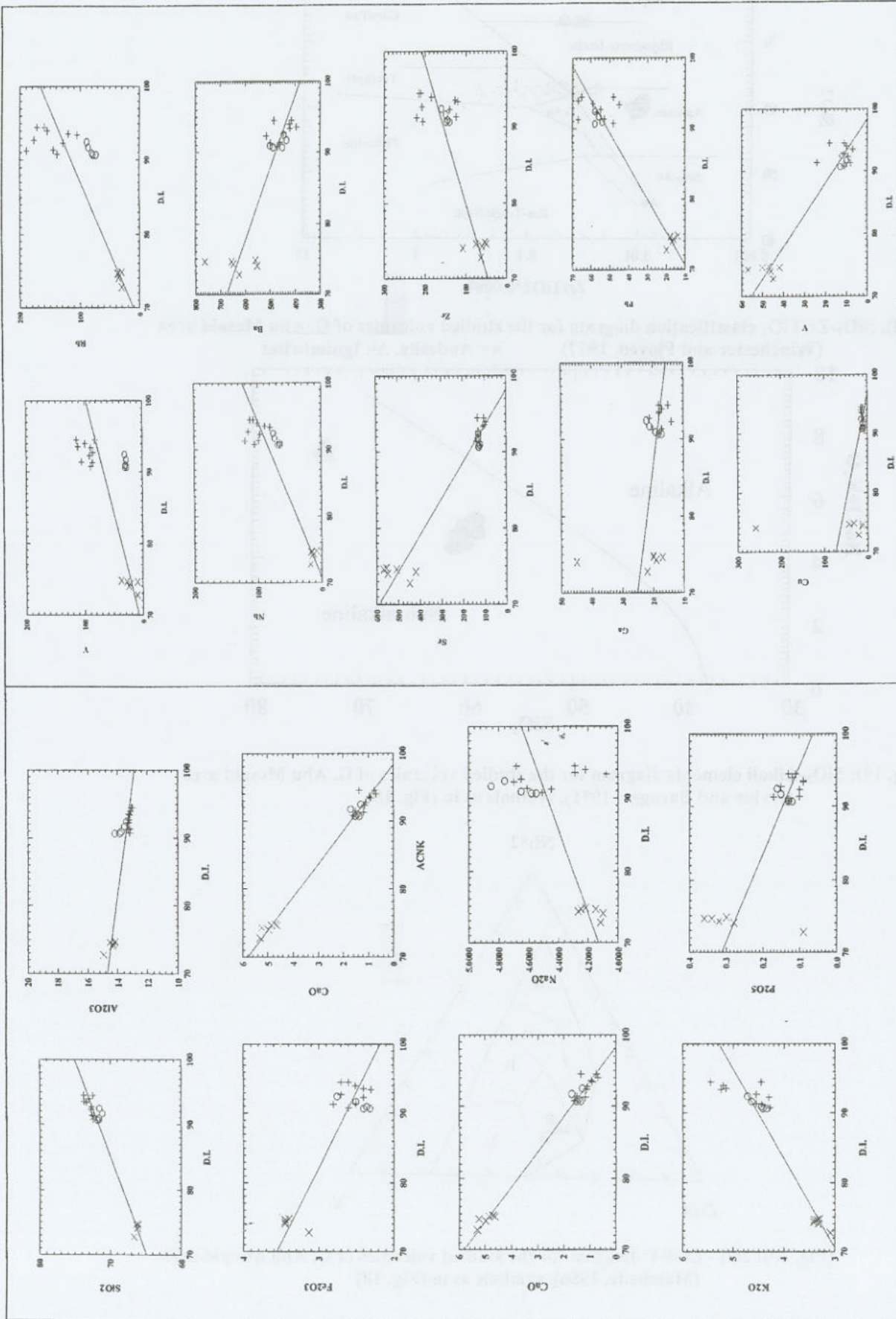
(Fig. 18): SiO₂-Zr/TiO₂ classification diagram for the studied volcanics of G. Abu Mesaid area (Winchester and Floyd, 1977) ● = Andesite, Δ = Ignimbrites



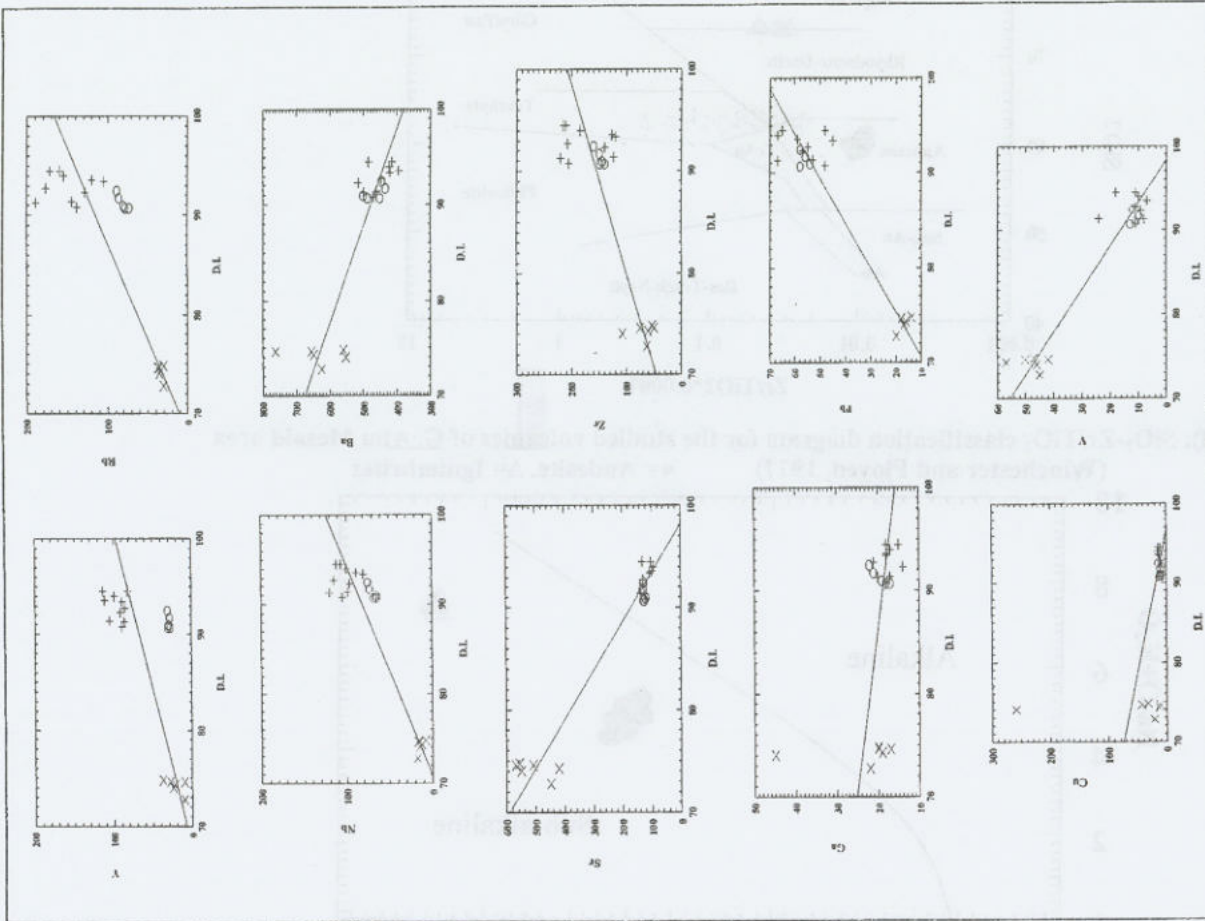
(Fig. 19): SiO₂-Alkali elements diagram for the studied volcanics of G. Abu Mesaid area (Irvine and Baragar, 1971), symbols as in (Fig. 18)



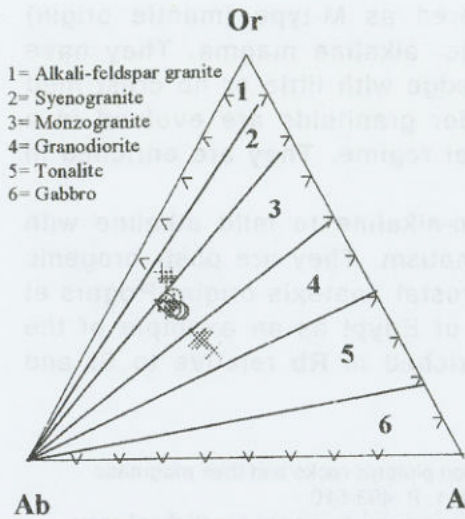
(Fig. 20): 2Nb- Zr/4-Y diagram for the studied volcanics of G. Abu Mesaid area (Meschede, 1986), symbols as in (Fig. 18)



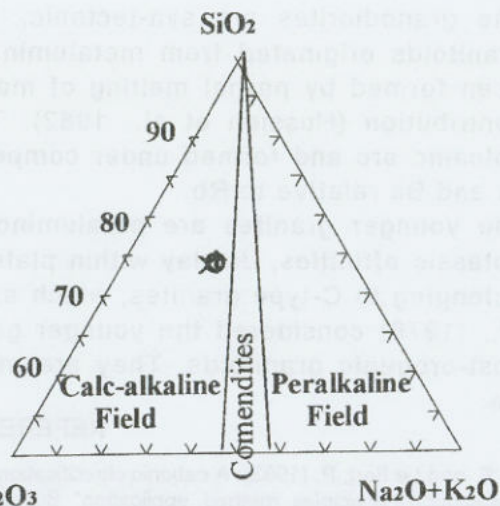
(Fig. 21): Major oxides vs D.I. variation diagrams for the studied granites of G. Abu Mesaid area. x=Granodiorite, +=Biotite granite, o=Hornblende granite



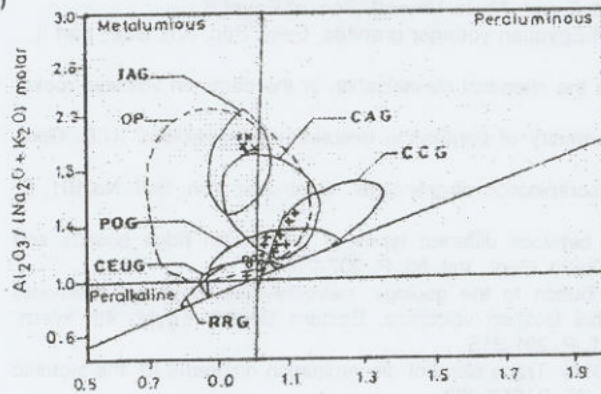
(Fig. 22): Trace elements vs D.I. variation diagrams for the studied granites of G. Abu Mesaid area. Symbols as in (Fig. 21).



(Fig. 23): Or-An- Ab classification diagram for the studied granites of G. Abu Mesaid area (Streckeisen, 1976), 21)



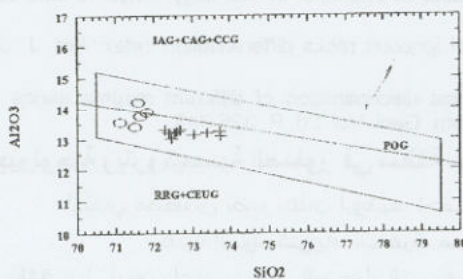
(Fig. 24): SiO₂- Al₂O₃- Na₂O+K₂O ternary diagram for the studied granites of G. Abu Mesaid area (Mac- symbols as in (Fig. Donald and Baily, 1976), symbols as in (Fig. 21)



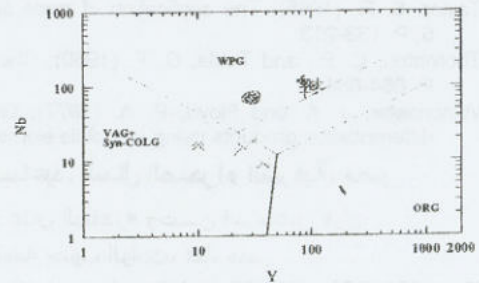
(Fig. 25): Shand's index discrimination diagram for the studied granites of G. Abu Mesaid area (Maniar and Piccoli, 1989), symbols as in (Fig. 21)

Orogenic granitoid rocks
 IAG= Island arc granitoids.
 CAG= Continental arc granitoids.
 CCG= Continental collision granitoids.
 POG= Post-Orogenic granitoids.

Anorogenic granitoid rocks
 RRG= Rift-related granitoids.
 OP= Oceanic plagiogranite.
 CELUG= Continental epirogenic Granitoids.



(Fig. 26): SiO₂-Al₂O₃ discrimination diagram for the studied granites of G. Abu Mesaid area (Maniar and Piccoli, 1989), symbols as in (Fig. 21)



(Fig. 27): Y-Nb discrimination diagram for the studied granites of G. Abu Mesaid area (Pearce, 1984), symbols as in (Fig. 21)

4- The granitoid rocks of the studied area comprise older granitoids and younger granites, they show considerable changes in chemical composition. The former are classified as granodiorites, while the latter are classified into syenogranites (biotite granites) and monzogranites (hornblende-biotite granites).

- 5- The granodiorites are syn-tectonic, considered as M-type (mantle origin) granitoids originated from metaluminous calc-alkaline magma. They have been formed by partial melting of mantle wedge with little or no crust melt contribution (Hussien et al., 1982). The older granitoids are evolved in a volcanic arc and formed under compressional regime. They are enriched in Sr and Ba relative to Rb.
- 6- The younger granites are peraluminous calc-alkaline to mild alkaline with potassic affinities, display within plate magmatism. They are post-orogenic belonging to C-type granites, which are of crustal anatexis origin. Rogers et al., (1978) considered the younger granites of Egypt as an example of the post-orogenic granitoids. They are more enriched in Rb relative to Sr and Ba.

REFERENCES

- Debon, F. and Le Fort, P. (1983): A cationic classification of common plutonic rocks and their magmatic association's principles, method, application". Bull. Min., Vol. 111, P. 493-510.
- El Kholi, D. M.; Ammar, F. A. and El Galy, M. M. (1998): Geology, geochemistry and radioactivity of some granitoid rocks, Northwest Hurghada area, Eastern Desert, Egypt. Al-Azhar Bull. Sci. Vol. 9, No. 2, P. 289-313.
- EL-Sharkawy, M. A. Abu Zied, H. T.; EL Bayoumi, R. M.; Shaalan, M., and Khalaf, E. A.H. (1991): On the volcanic rocks of Gabal Dokhan, Eastern Desert, Egypt. Abstr. Mineral. Soc. of Egypt.6.
- Greenberg, J. K. (1981): Characteristics and origin of Egyptian younger granites. Geol. Soc. Am. Bull., part II, Vol. 92, P. 749-840.
- Irvine, T. N. and Baragar, W. A., (1971): A guide to the chemical classification of the common volcanic rocks. Can. J. Earth Sci., 8, P. 523-548.
- Mac Donald, R. and Bailey, D. K. (1973): The chemistry of peralkaline oversaturated obsidians .U.S. Geol. Surv. Prof. Pap. 44- No.1, P. 37.
- Maniar, P. D. and Piccoli, P. M. (1989): Tectonic discrimination of granitoids. Geol. Soc. Am. Bull. No.101, P. 635-643.
- Meschede, M. (1986): A method of discriminating between different types of mid ocean ridge basalts and continental tholeiites with the Nb -Zr-Y diagram. Chem. Geol., Vol. 56, P. 207-218.
- Nossair, L. M. and El Galy, M. M. (1999): Contribution to the geology, petrochemistry and radioelements distribution of the granitic rocks intruding Gabal Dokhan volcanics, Eastern Desert, Egypt: 4th intern. Conf. On Geochemistry, Alex. Univ., Egypt, Vol. 1, P. 291-315
- Pearce, J. A.; Harris, N. B. W. and Tindle, A. G. (1984): Trace element discrimination diagrams for the tectonic interpretation of granitic rocks. J. Petrology., Vol. 25, P. 956-983.
- Streckeisen, A. (1976): Classification of common igneous rocks by means of their chemical composition. A provisional attempt. N. Jb. Mineral. Mh., H.I., 1-15.
- Taylor, S. R. (1965): The application of trace element data to problems in petrology. Phys. Chem. Earth. Vol. 6, P. 133-213.
- Thornton, C. P., and Tuttle, O. F. (1960): Chemistry of igneous rocks differentiation index. Am. J. Sec., 258, P. 664-684.
- Winchester, J. A. and Floyd, P. A. (1977): Geochemical discrimination of different magma series and their differentiation products using immobile elements, Chem. Geol. Vol. 20, P. 325-343.

جيولوجية وبتروكيميائية الصخور في منطقة جبل أبو مساعيد، شمال الصحراء الشرقية، مصر

لطفي مصطفى نصير، علي أبوضيف أحمد، محمد علي الطاهر* وحسن اسماعيل فراج

هيئة المواد النووية، القاهرة، مصر - *جامعة جنوب الوادي، قنا، مصر

تقع منطقة جبل أبو مساعيد بشمال الصحراء الشرقية المصرية بين خطي الطول 15° 33' و 22° 33' شرقاً وخطي العرض 17° 27' و 26° 27' شمالاً، وتغطي مساحة قدرها 160 كم² تقريباً. تعتبر صخور الجرانودايورايت من أقدم الصخور الجرانيتية في المنطقة وهي تغطي جزءاً صغيراً بالجانب الشرقي من المنطقة. هذه الصخور غالباً ما تقطع بحدود حامضية وقاعدية. تغطي صخور بركانيات الدخان جزءاً كبيراً من المنطقة وتتراوح في التركيب من الأنديزيت إلى الريبوليت ومصاحبتها من الصخور البركانية الفتاتية، تنتمي هذه البركانيات إلى أقواس جزر كاملة النضج. يغطي الجرانيت الحديث حوالي 40-50% من منكشفات منطقة البحث متمثلاً بالكتلة الجرانيتية التي تكون جبل أبو مساعيد. وقد أوضحت الدراسة الحقلية وجود نوعين من الجرانيت الحديث هما الجرانيت البيوتيتي والجرانيت الهورنبلندي البيوتيتي. تم عمل تحاليل كيميائية للصخور المختلفة بالمنطقة قيد الدراسة حيث أوضحت هذه الدراسات أن الجرانيت القديم هو من نوع (I) الميتاألوميني ذو الأصل الوشاحي وهو من الصخور الكلس - قلوية والذي ينتمي إليه غالبية الجرانيت المصري القديم. أما صخور بركانيات الدخان فوجد أن خواصها الكيميائية تماثل بركانيات السلسلة الكلس - قلوية. أما صخور الجرانيت الحديث فهي تكون سلسلة ذات طبيعة فوق ألومينية وتدرج من الكلس - قلوية إلى القلوية وهي لها ميل بوتاسي.